Splitting Phenomena in Wave Packet Propagation

I. A. Valuev[1] and B. Esser[2]

[1] Moscow Institute of Physics and Technology,
Department of Molecular and Biological Physics,
141700 Dolgoprudny, Russia
valuev@physik.hu-berlin.de
[2] Institut für Physik, Humboldt-Universität Berlin,
Invalidenstrasse 110, 10115 Berlin, Germany
besser@physik.hu-berlin.de
http://www.physik.hu-berlin.de

Abstract. Wave packet dynamics on coupled potentials is considered on the basis of an associated Spin-Boson Hamiltonian. A large number of eigenstates of this Hamiltonian is obtained by numerical diagonalization. Eigenstates display a mixing of adiabatic branches as is evident from their Husimi (quantum density) projections. From the eigenstates time dependent Husimi projections are constructed and packet dynamics is investigated. Complex packet dynamics is observed with packet propagation along classical trajectories and an increasing number of packets due to splitting events in the region of avoided crossings of these trajectories. Splitting events and their spin dependencies are systematically studied. In particular splitting ratios relating the intensities of packets after a splitting event are derived from the numerical data of packet propagation. A new projection technique applied to the state vector is proposed by which the presence of particular packets in the evolution of the system can be established and made accessible to analysis.

1 Introduction and Model

Wave packet dynamics is one of the central topics in quantum evolution with a wide range of applications ranging from from atomic and molecular physics to physical chemistry (see e.g. [1] and references therein). We present a numerical investigation of the dynamics of wave packets in a many-potential system, when phase space orbits associated with different adiabatic potentials are coupled. Basic to our investigation is the evolution of quantum states described by the Spin-Boson Hamiltonian

$$\hat{H} = \epsilon_+ \hat{1} - \frac{1}{2}\hat{\sigma}_x + \frac{1}{2}(\hat{P}^2 + r^2\hat{Q}^2)\hat{1} + (\sqrt{\frac{p}{2}} r\hat{Q} + \epsilon_-)\hat{\sigma}_z. \tag{1}$$

In (1) a quantum particle residing in two states is coupled to a vibrational environment specified by the coordinate Q. The two state quantum system is

P.M.A. Sloot et al. (Eds.): ICCS 2002, LNCS 2331, pp. 1184–1192, 2002.

represented by the standard Pauli Spin Matrices $\hat{\sigma}_i$ $(i = x, z)$, r is the dimensionless vibrational frequency of the oscillator potential and p is the coupling constant between the dynamics of the particle and the vibrational environment. We note that (1) is a generalized Spin-Boson Hamiltonian containing the parameter ϵ_- , which destroys the parity symmetry of the eigenstates of the more conventional Spin-Boson Hamiltonian in which such a term is absent.

A Hamiltonians like (1) can be obtained from different physical situations, the particle being e.g. an electron, exciton or any other quasiparticle. To be definite we will use a "molecular" language and consider the situation when the Hamiltonian (1) is derived from a molecular physics model. We consider a molecular dimer, in which the transfer of an excitation between two monomers constituting the dimer and coupled to a molecular vibration is investigated. Then ϵ_- is the difference between the energies of the excitation at the two non-equivalent monomers constituting the dimer (ϵ_+ in (1) is the mean excitation energy, in what follows we omit this term thereby shifting the origin of the energy scale to ϵ_+). For the details of the derivation of (1) from a molecular dimer Hamiltonian and in particular the connection between the dimensionless parameters of (1) with a dimer model we refer to [2] and references therein.

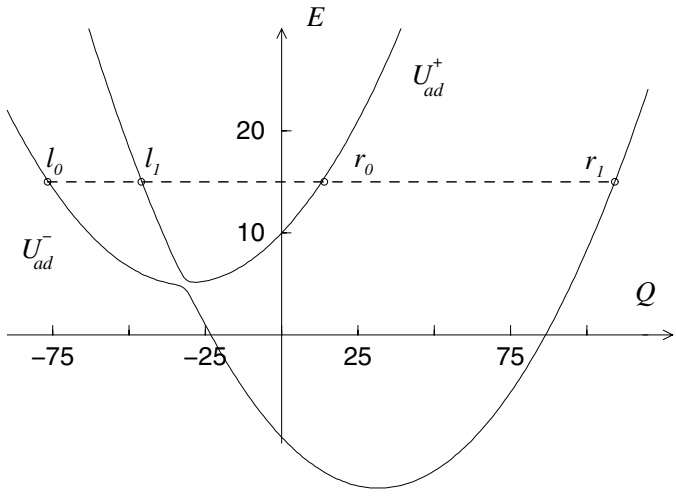

Fig. 1. Adiabtic potentials for the parameter set used. The line of constant energy $E = 15$ and its crossing points with the potentials (turning points) are shown. The turning points are labeled according to the location of the point (l for "left" and r for "right") and monomer (spin) indicies 0 and 1 correspond to the upper and lower monomer, respectively

Applying a Born - Oppenheimer stepwise quantization to (1) one obtains the Hamiltonians of the adiabatic reference systems

$$H^{\pm}(Q) = \frac{1}{2}P^2 + U_{\mathrm{ad}}^{\pm}(Q). \tag{2}$$

with the adiabatic potentials

$$U_{\mathrm{ad}}^{\pm}(Q) = \frac{r^2}{2}Q^2 \pm \sqrt{\frac{1}{4} + \left(\epsilon_- + \sqrt{\frac{p}{2}}rQ\right)^2}\,, \tag{3}$$

In Fig. 1 the adiabatic potentials for a given parameter set are shown. Fixing an energy E phase space orbits can be derived from (2) for each of the adiabatic potentials. Phase space trajectories of isolated monomers at a given energy E can be derived in an analogous way by neglecting the quantum transfer in (1) (discarding $\hat{\sigma}_x$). In what follows we denote the upper and lower monomer of the dimer configuration by the indices (0) and (1), respectively. In spin representation projections of the state vector on such monomer states correspond to projections on the spin up state (upper monomer) and spin down state (lower monomer), respectively. We note that in the semiclassical case adiabatic trajectories can be represented as built from pieces of monomer trajectories. In the analysis of packet propagation derived from the state vector it will be convenient to use projections on such monomer states below.

A quantum density in phase space is constructed by using Husimi projections extended by spin variables. For a given state vector $|\Psi\rangle$ such densities are derived by projecting $|\Psi\rangle$ on a combined basis of standard coherent oscillator states $|\alpha(Q,P)\rangle$, which scan the phase space plane Q, P, multiplied by spin states $|s\rangle$, $|s\rangle = c_\uparrow|\uparrow\rangle + c_\downarrow|\downarrow\rangle$ via

$$h_\Psi(\alpha(Q,P);s) = |\langle\,\Psi\mid\alpha(Q,P),s\rangle|^2. \tag{4}$$

Husimi densities are equivalent to Gaussian smoothed Wigner distributions, positive definite and useful in phase space analysis of quantum states [3]. Here we will use Husimi densities to analyze wave packet dynamics.

2 Numerical procedure and phase space density

A large number of eigenstates and eigenvalues of (1) was obtained by a direct matrix diagonalization method for different parameters p, r and ϵ_- using the ARPACK package [4]. For the matrix diagonalization a basis of the harmonic oscillator eigenstates extended by the spin variable was used. Here we report results for the particular parameter set $p = 20$, $r = 0.1$ and $\epsilon_- = 10$, for which a diagonalization of a matrix of dimension $N = 4000$ was applied. From this diagonalization the first 1100 eigenvalues and eigenvectors were used in constructing the statevectors.

The Husimi density of a representative eigenstate computed from an eigenvector using (4) is shown in the Fig. 2, where the classical phase space orbits corresponding to the adiabatic potentials at the energy of the eigenvalue of the selected eigenstate are included. From Fig. 2 it is seen that the eigenstate density is located on both of the adiabatic branches, i.e. adiabatic branches are mixed in the eigenstates of (1).

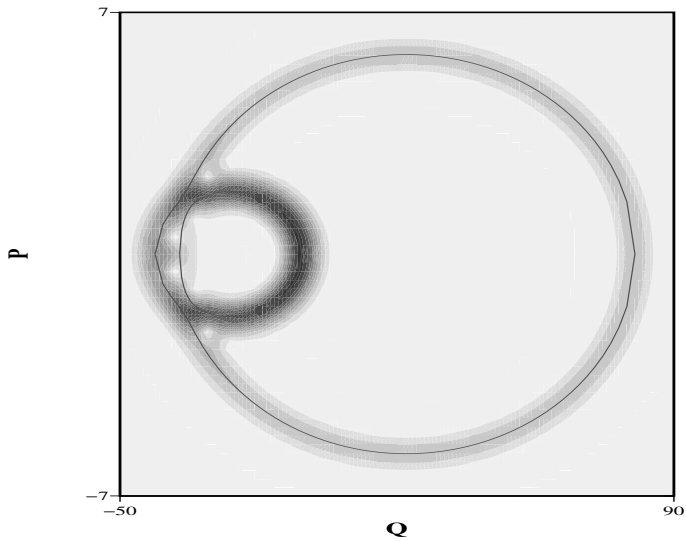

Fig. 2. Husimi distribution of the eigenstate number 184. The quantum phase space density is located on both of the adiabatic branches, the corresponding classical phase space orbits of which are shown as lines

A detailed analysis of sequences of such eigenstates [2], shows that the components of this density, located on a given adiabatic branch change from one eigenstate to another in a rather irregular fashion. This mixing of adiabatic branches in the spectrum of (1), which can be shown by different methods, such as e.g. Bloch projections [5], can be viewed as appearance of spectral randomness and is well known as incipience of quantum chaos [6], when the random features of the spectrum just appear, but regular parts of the spectrum are still intact. Quantum and classical consequences of this behaviour of the Spin-Boson Model have been intensively investigated over the last years [7], [8], [9].

Here we address the dynamical consequences of the mixing of adiabatic branches of the spectrum of (1) for the particular phenomenon of wave packet splitting. As a result of this mixing splitting events of wave packets initially prepared on one adiabatic branch will occur and packets propagating on different branches appear. This can be observed by using Husimi projections constructed from a time dependent state vector $|\Psi(t)\rangle$ in (4).

3 Splitting analysis of packet propagation

We investigated packet dynamics by propagating numerically test wave packets, which can be constructed initially at the arbitrary positions (Q_0, P_0) in phase space as coherent states multiplied by the initial spin $|\psi(0)\rangle = |\alpha(P_0, Q_0)\rangle|s_0\rangle$. Then time propagation of the state vector $|\Psi(t)\rangle$ corresponding to the initial condition was performed by using the numerically obtained eigenstates and eigen-

values. Packet propagation was analyzed in detail by means of Husimi projections (4). In the Fig. 3 a snapshot of such a packet propagation for an initial packet placed at the left turning point of the upper monomer potential with an energy $E = 12$ is shown. The snapshot is taken at the moment $t = 1.1(2\pi/r)$, i. e. for $t = 70$, below the time unit $2\pi/r$ (free oscillator period) is everywhere indicated.

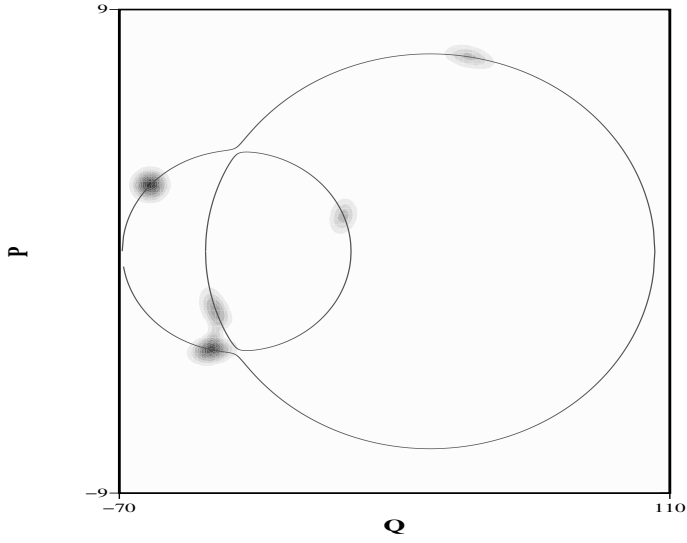

Fig. 3. Snapshot of wave packet propagation at a time $t = 1.1(2\pi/r)$ for an initial wave packet placed at the left turning point of the left monomer (0), energy E=12. For comparison the adiabatic phase space trajectories at the same energy are shown. In the left lower part a splitting event is observed. In the Husimi density the projection spin is equal on both monomers

We observed splitting phenomena of propagated wave packets at each of the crossing points of the monomer phase space trajectories. The region of such crossing points of monomer phase space trajectories is equivalent to the avoided crossings of the adiabatic trajectories shown in the Fig. 3 (in what follows for shortness we will refer to this phase space region simply as monomer crossings). In the Fig. 3 a splitting event is visible in the left lower part of the phase space near such a crossing. The intensity of the propagated and split wave packets was considered in dependence both on the energy E and the spin projection. Packets with spin projections corresponding to the phase space trajectory of the monomer on which propagation occurs turned out to be much more intensive than packets with opposite spin projections (for the parameter set used the intensity ratio was approximately three orders of magnitude). We call the much more intensive packets, for which spin projection corresponds to the monomer phase space trajectory, main packets and the other packets "shadow" packets.

When a main packet reaches a crossing point it splits into two main packets, one main packet propagating on the same monomer phase space trajectory as before, and the other main packet appearing on the trajectory of the other monomer. Both packets then propagate each on their own monomer trajectory with approximately constant Husimi intensities until they reach the next crossing point. Then the packets split again, etc. The result of several splittings of this kind is seen from Fig. 3.

Splitting events can be classified as primary, secondary and so on in dependence of their time order. For a selected initial condition splitting events can be correspondingly ordered and classified into a splitting graph. We present such a splitting graph in the Fig. 6(a), where as a starting point the left turning point of the lower monomer potential and the energy $E = 15$ were used.

In order to minimize the amount of data to be analyzed for packet propagation and splitting events we developed a turnpoint analysis and a numerical program. This program monitors the Husimi intensities of all of the packets resulting from splitting events, when they cross any of the turning points in dependence on their spin projections. The initial packet was also placed at a turning point of a monomer phase space trajectory.

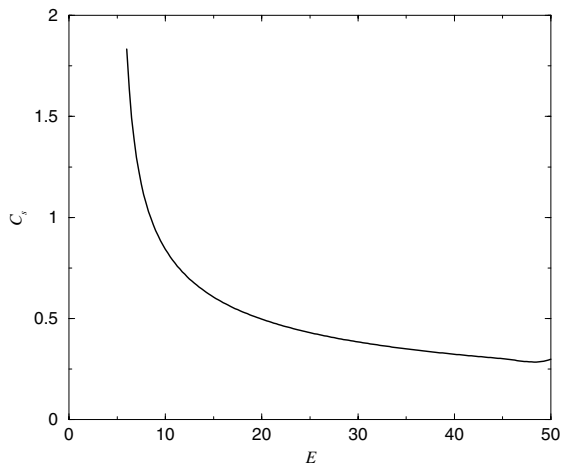

Fig. 4. Splitting coefficient C_s measured as the ratio of the Husimi projections of the packets passing the corresponding turning points after splitting (see text)

First of all we investigated the Husimi intensity for the primary splittings by considering the four turning points as initial conditions for such splitting processes. According to our turnpoint analysis procedure these primary splittings can be classified as follows:

$$\begin{aligned}
\{l_0, u\} &\Rightarrow \{r_1, d\},\ \{r_0, u\} \\
\{r_0, u\} &\Rightarrow \{l_1, d\},\ \{l_0, u\} \\
\{l_1, d\} &\Rightarrow \{r_0, u\},\ \{r_1, d\} \\
\{r_1, d\} &\Rightarrow \{l_0, u\},\ \{l_1, d\}
\end{aligned}$$

Here on the left sides of the arrows the positions of the initial packets and on the right sides of the two final packets at their turning points are indicated as 0 for the upper and 1 for the lower monomer, respectively. The letters l, r denote the left, right turning points (see Fig. 1), and spin indices u, d the up and down projections. For shortness here the main packets are considered, when all the projection spins correspond to the turning points of "their" monomer trajectory. In the turnpoint analysis the energy was changed over a broad interval in which well defined packets are present and the Husimi intensities measured. The analysis of the obtained data showed that the ratio C_s of the intensity of the packet that appears on the other monomer trajectory to the intensity of the packet that remains on the initial monomer trajectory after a splitting is constant for all primary splitting configurations and is a function of the initial packet energy only (Fig. 4).

All the packets observed in the propagation are due to complex interference inside the state vector $\Psi(t)$ of the system. In order to investigate this complex behaviour we introduced special projection states with which it is possible to analyze the process of appearance of packets. Such projection states can be introduced by an artificially constructed state vector

$$|M(t)\rangle = \sum_i a_i |\alpha(Q_i(t), P_i(t))\rangle |s_i\rangle, \tag{5}$$

which is a superposition of coherent states modelling all packets at a given time t. The packets are indexed by i and contribute to $|M(t)\rangle$ with their coefficients a_i and spin $|s_i\rangle$ that corresponds to the monomer trajectory the packet is propagating on. The coefficients a_i can be derived from the splitting data of the turnpoint analysis. The phase space positions $(Q_i(t), P_i(t))$ are chosen according to the semiclassical motion of the packet centers. We note that this construction provides only the amplitudes a_i (all a_i are assumed to be real), because information about the phases cannot be extracted from the Husimi densities. For an initial packet in $|M(t)\rangle$ chosen to be the same as for the exact quantum propagation, it is possible to investigate the correspondence between the reference states $|M(t)\rangle$ and the exact state vector $|\Psi(t)\rangle$.

A comparison of the correlation functions $\langle\Psi(0)|\Psi(t)\rangle$ and $\langle M(0)|M(t)\rangle$ shows very similar reccurence features (Fig. 5). The intensities of the reccurence peaks for the exact and model wavefunctions are in good agreement at the early stage of propagation. The reccurence times are in agreement even for longer propagation times, when a lot of packets already exist in the splitting model based on (5) (1584 packets for $t = 5(2\pi/r)$ in Fig. 5).

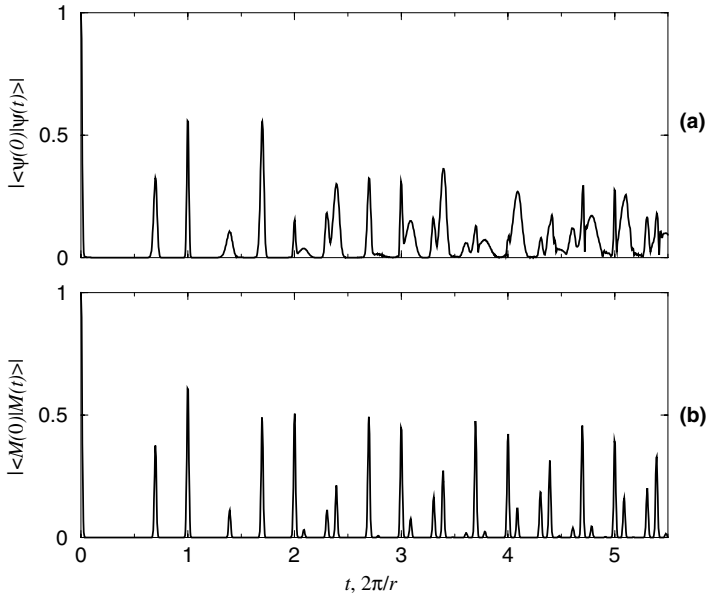

Fig. 5. The correlation functions for the initial packet located at the turning point l_1 with initial spin $|\downarrow\rangle$ and $E = 15$: (a) – from numerical propagation and (b) – from the splitting model. Time is measured in periods of the osillator associated with monomers

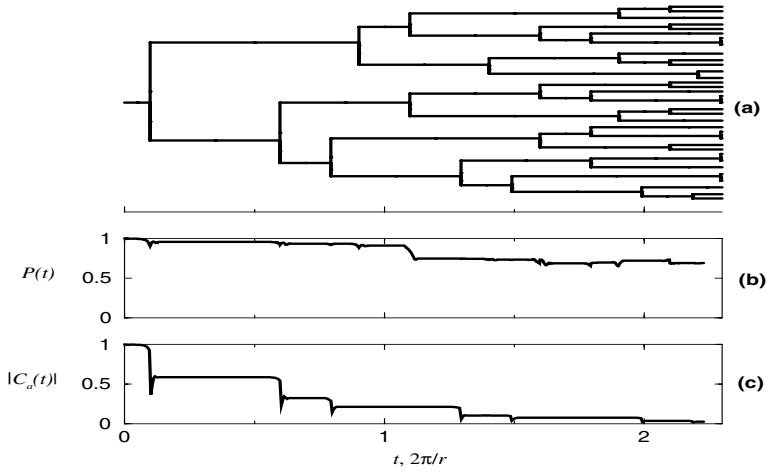

Fig. 6. The splitting dynamics of the state initially located at the turning point l_1 with initial spin $|\downarrow\rangle$ and $E = 15$. (a) Splitting event graph. The branchings correspond to splittings of the packets, the packets which change and do not change the monomer trajectory are displayed by the lines going down and up, respectively. (b) Correlation of the numerically propagated wavefunction and the normalized splitting model wavefunction. (c) Correlation of the numerically propagated wavefunction and the packet, classically moving along the lower adiabatic potential

For direct comparison of $|M(t)\rangle$ and $|\Psi(t)\rangle$ we use the sum of projections of all packets existing in $|M(t)\rangle$ on $|\Psi(t)\rangle$:

$$P(t) = \sum_i a_i |\langle\Psi(t)|\alpha(Q_i(t), P_i(t))\rangle|s_i\rangle|. \tag{6}$$

From the Fig. 6(b), where $P(t)$ is presented it is seen that $|M(t)\rangle$ is a good approximation to the state vector $|\Psi(t)\rangle$. This shows that this projection technique offers a possibility to analyze the exact state vector.

The projection of an individual reference packet moving classically along some phase space trajectory, for example the trajectory of an adiabatic potential, on $|\Psi(t)\rangle$ can be used to find out to what extent this packet is contained in the time evolution. The projection of this type, $C_a(t) = \langle M_a(t)|\Psi(t)\rangle$, where $|M_a(t)\rangle$ is the model wavefunction constructed from a packet of constant intensity moving along the lower adiabatic potential without splittings, is shown in Fig. 6(c). The initial state for both the exact state vector and the reference state $|M_a(t)\rangle$ is the same and located in the turning point l_0. The absolute value of $C_a(t)$ decays stepwise as the splittings in $|\Psi(t)\rangle$ occur.

We conclude that the construction of reference states $|M(t)\rangle$ captures essential features of wave packet propagation and splitting displayed by the exact state vector $\Psi(t)$ and therefore can be used for wave packet modelling and projection techniques. Following this idea we can make the birth process of packets in the splitting region accessible to direct investigation by projecting the exact state vector on such reference states. Using particular spin states for $|\alpha(Q_i(t), P_i(t))\rangle|s_i\rangle$ in projections, it should be possible to project out the birth processes of packets in the state vector $|\Psi(t)\rangle$ in the splitting region.

Acknowledgements

Financial support from the Deutsche Forschungsgemeinschaft (DFG) is gratefully acknowledged.

References

1. J. E. Bayfield, Quantum Evolution, John Wiley and Sons Inc., New York 1999.
2. C. Koch and B. Esser, Phys. Rev. A 61, 22508 (2000).
3. K. Takahashi, Progr. Theor. Phys. Suppl. 98, 109 (1989).
4. R. B. Lehoucq, D. C. Sorensen and C. Yang, Arpack Users Guide: Solution of Large Scale Eigenvalue problems, http://www.caam.rice.edu/software/ARPACK
5. H. Schanz and B. Esser, Z. Phys. B 101, 299 (1996).
6. M. Cibils, Y. Cuche, and G. Müller, Z. Phys. B 97, 565 (1995).
7. L. Müller, J. Stolze, H. Leschke, and P. Nagel, Phys. Rev. A 55, 1022 (1991).
8. H. Schanz and B. Esser, Phys. Rev. A 44, 3375 (1997).
9. R. Steib, J. L. Schoendorff, H. J. Korsch, and P. Reineker, Phys. Rev. E 57, 6534 (1998).